



Dissipative Dicke time crystals: an atoms' point of view

Simon B. Jäger , Jan Mathis Giesen, Imke Schneider, and Sebastian Eggert 
*Physics Department and Research Center OPTIMAS,
 University of Kaiserslautern-Landau, D-67663, Kaiserslautern, Germany*

We develop and study an atom-only description of the Dicke model with time-periodic couplings between atoms and a dissipative cavity mode. The cavity mode is eliminated giving rise to effective atom-atom interactions and dissipation. We use this effective description to analyze the dynamics of the atoms that undergo a transition to a dynamical superradiant phase with macroscopic coherences in the atomic medium and the light field. Using Floquet theory in combination with the atom-only description we provide a precise determination of the phase boundaries and of the dynamical response of the atoms. From this we can predict the existence of dissipative time crystals that show a subharmonic response with respect to the driving frequency. We show that the atom-only theory can describe the relaxation into such a dissipative time crystal and that the damping rate can be understood in terms of a cooling mechanism.

Time-periodic driving of quantum systems allows for the creation of tailored out-of-equilibrium structures including quantum states with topological order [1, 2] and self-organized coherent patterns [3–9]. Here, one distinguishes between off-resonant driving and resonant driving. In the high frequency limit, the former results in a quasi static quantum system that experiences an engineer-able and time-averaged Hamiltonian [10, 11]. Resonant driving, instead, enables strong dynamical coherences between otherwise weakly coupled quantum states which can force the quantum system in exotic spatio-temporal pattern. This is exciting as it allows the controlled, on-demand generation of purpose-oriented quantum states but comes at the cost of inserting large amounts of energy into the system which can lead to heating and eventually coherence loss. A possible cure to this problem is the use of engineered dissipation [12, 13] which is designed to drain away excess energy and damp the system into a coherent limit cycle.

To study such mechanisms the time-periodic dissipative Dicke model describing the time-modulated interaction of atoms with a cavity is a rich prototypical platform. In this setup periodic driving can induce the formation of subharmonic spatio-temporal pattern, so called dissipative time crystals, which are accompanied by superradiant light emission into the cavity and were recently the focus of several experimental and theoretical works [13–19]. While the interest mostly lies in the evolution of the atomic configuration, the cavity is crucial in two ways [20–22]: (i) it mediates tunable time-periodic atom-atom interactions which are essential for the pattern formation and (ii) it opens a dissipative channel which can drain energy introduced by the drive. The onset of the spatio-temporal structure can be understood from (i) the time-periodic modulation of the interactions that can induce a parametric resonance in the atomic ensemble [14, 23, 24]. However, the stabilization of the emerging pattern can only be explained by the presence of (ii) the cavity-generated dissipation which makes an ad-hoc elimination of the cavity difficult [13]. Espe-

cially in the limit of strong atom-photon interaction it seems therefore natural to treat the dynamics of atoms and cavity on equal footing, which is the usual approach. However, as we show in this Letter it is possible to completely eliminate the photons even for periodically-driven systems. The resulting atom-only description has several advantages [25, 26]: it allows the detailed study not only of the non-equilibrium phase diagram, but also of the full evolution towards stable limit cycles. In return, it is possible to get a much deeper insight in the dissipation mechanism of the atomic degrees of freedom, which stabilize the spatio-temporal patterns. Moreover, it allows an analytical description in terms of Floquet theory for large systems and paves the way for future engineering of tailored dynamic atomic models, which can be used as quantum simulators of complicated interacting systems.

Model– We consider the time-periodic dissipative Dicke model and eliminate the cavity in order to derive an effective atom-only Master equation which is of Lindblad form [27]. The dynamics of the density operator $\hat{\rho}$ describing the atoms and one coupled cavity mode with loss rate κ is governed by the master equation ($\hbar = 1$)

$$\frac{\partial \hat{\rho}}{\partial t} = -i [\hat{H}, \hat{\rho}] - \kappa (\hat{a}^\dagger \hat{a} \hat{\rho} + \hat{\rho} \hat{a}^\dagger \hat{a} - 2\hat{a} \hat{\rho} \hat{a}^\dagger). \quad (1)$$

The coupling to N two-level atoms that are driven by an external laser is described by the Hamiltonian [28, 29]

$$\hat{H} = \delta_c \hat{a}^\dagger \hat{a} + \Delta \hat{n}_\uparrow + \frac{g(t)}{\sqrt{N}} (\hat{a} + \hat{a}^\dagger) (\hat{b}_\uparrow^\dagger \hat{b}_\downarrow + \hat{b}_\downarrow^\dagger \hat{b}_\uparrow), \quad (2)$$

where δ_c is the detuning between the cavity resonance and the external laser drive, \hat{a}^\dagger and \hat{a} are the cavity field creation and annihilation operators, and the bosonic operators $\hat{b}_\uparrow^\dagger \hat{b}_\downarrow$ change one atomic state from the ground state $|\downarrow\rangle$ to the metastable excited state $|\uparrow\rangle$ of energy Δ . The operators $\hat{n}_\uparrow = \hat{b}_\uparrow^\dagger \hat{b}_\uparrow$ and $\hat{n}_\downarrow = \hat{b}_\downarrow^\dagger \hat{b}_\downarrow$ measure the number of atoms in each state such that $N = \hat{n}_\uparrow + \hat{n}_\downarrow$. A modulation of the external driving laser leads to a time-periodic collective coupling $g(t) = g_0 + g_1 \cos \omega t$, corresponding to two side-bands of the drive.

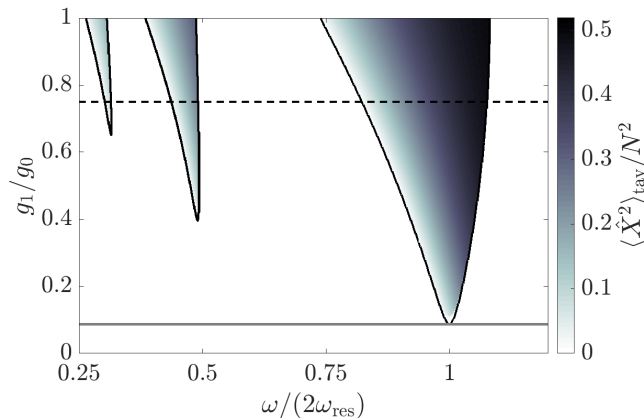


FIG. 1. The time-averaged superradiance order parameter $\langle \hat{X}^2 \rangle_{\text{tav}}$ calculated from the mean-field equations (7),(8) and evaluated at $\kappa t = 10^4$ as function of the driving frequency $\omega/(2\omega_{\text{res}})$ and driving strength g_1/g_0 . Curved solid lines mark the threshold to superradiance that are calculated from the stability analysis above which $\gamma_{\text{max}} > 0$. The horizontal gray solid line indicates the threshold g_1^c/g_0 given by Eq. (12). The dashed horizontal line shows the parameter visible in Fig. 3, $g_1 = 0.75g_0$. We used $\delta_c = \kappa$, $\Delta = 0.1\kappa$, $g_0 = 0.5g_c$.

In the static limit, $g_1 = 0$, the dissipative Dicke model [Eq. (1)] shows a transition from normal state to superradiance at $g = g_c = [\Delta(\delta_c^2 + \kappa^2)/(4\delta_c)]^{1/2}$ [30, 31]. Superradiance is signaled by macroscopic coherences in the atomic medium $\langle \hat{X}^2 \rangle \propto N^2$, $\hat{X} = \hat{b}_\uparrow^\dagger \hat{b}_\downarrow + \hat{b}_\downarrow^\dagger \hat{b}_\uparrow$, and a large cavity field $\langle \hat{a}^\dagger \hat{a} \rangle \propto N$. In this Letter, we focus on the subcritical regime to study the influence of time periodic driving with $g(t) < g_c$ at all times. In this situation, a dynamical superradiant configuration can still be found depending on the driving amplitude g_1 when the driving frequency ω is close to a parametric resonance [14]. In Fig. 1 we show our results for the regions of superradiance in parameter space spanned by g_1 and ω . The colorbar shows the time-averaged mean value of the superradiance order parameter $\langle \hat{X}^2 \rangle_{\text{tav}} = \int_t^{t+T} \langle \hat{X}^2(t) \rangle / T$ with $T = 2\pi/\omega$. A derivation of this phase diagram is shifted to a later point in this Letter.

Atom-only description– First, we will derive the atom-only description, by extending the theory of Ref. [27] and applying it for the first time to a time-dependent problem. In the limit of a short cavity relaxation time, $|\delta_c - i\kappa| \gg \Delta, \omega, g$, we apply a Schrieffer-Wolf transformation $\hat{D}(t) = \exp(\hat{a}^\dagger \hat{\beta}(t) - \hat{\beta}^\dagger(t) \hat{a})$ to eliminate the photonic degrees of freedom. The condition for decoupling the atoms from the cavity modes in the master equation leads to a *time-dependent* equation of the transformation operators $\hat{\beta}(t)$

$$i \frac{\partial \hat{\beta}}{\partial t} = (\delta_c - i\kappa) \hat{\beta} + \frac{g(t)}{\sqrt{N}} \left(\hat{b}_\uparrow^\dagger \hat{b}_\downarrow + \hat{b}_\downarrow^\dagger \hat{b}_\uparrow \right) + [\Delta \hat{n}_\uparrow, \hat{\beta}] \quad (3)$$

which is solved by $\hat{\beta}(t) = c_+(t) \hat{b}_\uparrow^\dagger \hat{b}_\downarrow + c_-(t) \hat{b}_\downarrow^\dagger \hat{b}_\uparrow$ in the

steady state. The resulting differential equation is discussed in the appendix, which yields an expansion

$$c_\pm(t) \approx -\frac{1}{\sqrt{N}} \left(\frac{g(t)}{\delta_c - i\kappa} + \frac{i\dot{g}(t)}{(\delta_c - i\kappa)^2} \mp \frac{\Delta g(t)}{(\delta_c - i\kappa)^2} \right), \quad (4)$$

where the first term corresponds to the quasi-static solution. With $\hat{\beta}$ we can then write the effective master equation for the atomic density operator $\hat{\rho}_{\text{at}} = \text{Tr}_{\text{cav}}[\hat{D}^\dagger \hat{\rho} \hat{D}]$ by tracing over the cavity degrees of freedom

$$\frac{\partial \hat{\rho}_{\text{at}}}{\partial t} = -i [\hat{H}_{\text{at}}, \hat{\rho}_{\text{at}}] - \kappa (\hat{\beta}^\dagger \hat{\beta} \hat{\rho}_{\text{at}} + \hat{\rho}_{\text{at}} \hat{\beta}^\dagger \hat{\beta} - 2\hat{\beta} \hat{\rho}_{\text{at}} \hat{\beta}^\dagger). \quad (5)$$

This atom-only description includes the coherent time evolution of the atoms governed by the Hamiltonian

$$\hat{H}_{\text{at}} = \Delta \hat{n}_\uparrow + \frac{g(t)}{2\sqrt{N}} \left(\hat{\beta}^\dagger [\hat{b}_\uparrow^\dagger \hat{b}_\downarrow + \hat{b}_\downarrow^\dagger \hat{b}_\uparrow] + \text{H.c.} \right). \quad (6)$$

The non-trivial time-dependence of $\hat{\beta}(t)$ therefore enters both the (i) cavity-mediated interactions in the second term of Eq. (6) and the (ii) cavity-generated dissipation $\propto \kappa$ in Eq. (5).

Formation of a stable atomic state– The resulting atomic theory in Eqs. (5) and (6) can be used for a quantum mechanical description of the complete dynamics of the bosonic state, which is the main tool for the results in this Letter. In particular, it should predict correctly the expectation values in time-averaged stationary states, which are also accessible via stochastic simulations as discussed in the appendix, where the atomic and photonic degrees of freedom are modelled as semiclassical fields. As shown in Fig. 2(a) the dynamics of $\langle \hat{X}^2(t) \rangle_{\text{tav}}$ calculated from the atomic master equation (solid) and the semiclassical simulation (dashed) with $N = 100$ both show the same evolution to the steady state corresponding to dissipative time crystal. The excellent agreement on short and on long timescales is a clear indication that the atom-only theory is valid and we have included the correct cavity-mediated interactions and dissipation. Note that it is far from trivial that the atomic state can evolve towards a dissipative time crystal without explicitly simulating the cavity degrees of freedom.

For very large atom numbers N the simulation of the atom-only master equation becomes very challenging since the dimension of the Liouvillian in Eq. (5) scales as N^4 . To provide an efficient method to describe the dynamics for very large N a mean-field description for $\varphi_s = \langle \hat{b}_s \rangle$, $s = \downarrow, \uparrow$ can be derived from Eq. (5) (see appendix)

$$\frac{d\varphi_\downarrow}{dt} = i \frac{V_0 - iV_1}{N} |\varphi_\uparrow|^2 \varphi_\downarrow + i \frac{V_0 + iV_1}{N} \varphi_\uparrow^2 \varphi_\downarrow^*, \quad (7)$$

$$\frac{d\varphi_\uparrow}{dt} = -i \left(\Delta - \frac{V_0 + iV_1}{N} |\varphi_\downarrow|^2 \right) \varphi_\uparrow + i \frac{V_0 - iV_1}{N} \varphi_\downarrow^2 \varphi_\uparrow^*. \quad (8)$$

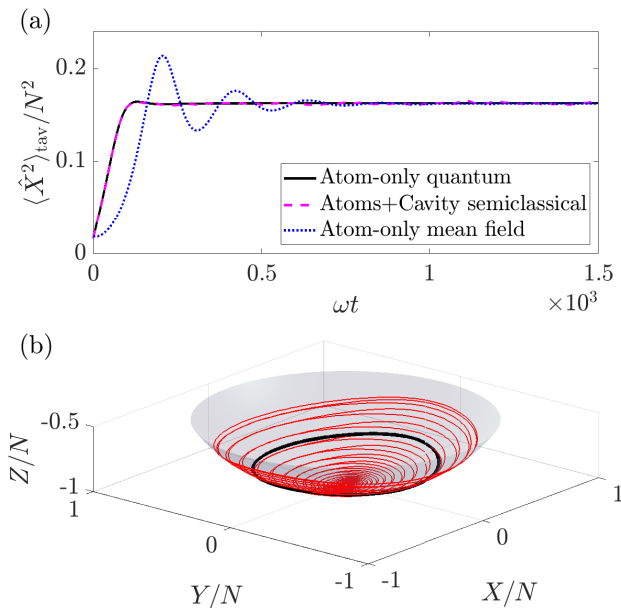


FIG. 2. The time-averaged observable $\langle \hat{X}^2 \rangle_{\text{tav}}$ as function of time for $N = 10^2$. The solid line is calculated from the atom-only effective master equation (5), the dashed line from the stochastic semiclassical simulation of atoms and cavity field, and the dotted line from the atom-only mean-field equations (7),(8). (b) Mean-field trajectory of $X(t), Y(t), Z(t)$ for $1.1 \times 10^3 \leq \omega t \leq 1.7 \times 10^3$ calculated from Eqs. (7),(8) with $V_1 \neq 0$ (black) and $V_1 = 0$ (red). The remaining parameters are $\delta_c = \kappa$, $\omega = 2\omega_{\text{res}}$, $g_0/g_c = 0.5$, $g_1/g_0 = 0.2$, and $\Delta = 0.1\kappa$.

This mean-field description includes (i) coherent interactions and (ii) dissipation that are described as non-linear terms proportional to $V_0 = -\sqrt{N}g(t)\text{Re}(c_+ + c_-)$ and $V_1 = N\kappa(|c_-|^2 - |c_+|^2)$, respectively. The amplitude c_- (c_+) describe the likelihood of atoms undergoing a transition from $|\uparrow\rangle$ to $|\downarrow\rangle$ ($|\downarrow\rangle$ to $|\uparrow\rangle$). An imbalance, in our case $N(|c_-|^2 - |c_+|^2) = 4\delta_c\Delta g^2(t)/(\delta_c^2 + \kappa^2)^2 > 0$ for $\Delta, \delta_c > 0$, leads to a preferential reduction of atomic excitations. Consequently, dissipation described by V_1 has a nice physical interpretation: it is a cooling rate which is crucial for the stabilization of the system over long timescales as we show below.

As shown in Fig. 2(a) the mean-field theory (dotted) evolves to the correct steady state for large times even for a modest value of $N = 100$. This is an important finding since the simple differential equations (7),(8) can be used to observe the relaxation towards a non-trivial stable dynamical state, which maps the whole phase diagram very efficiently in terms of the stationary mean field value $\langle \hat{X}^2 \rangle_{\text{tav}}/N^2$. The result is shown in Fig. 1. On short timescales we find an exponential growth and oscillations of the mean-field $\langle \hat{X}^2 \rangle_{\text{tav}}/N^2$ in Fig. 2(a) that is not visible in the quantum simulation of Eq. (5). The oscillations in the mean field value of $\langle \hat{X}^2 \rangle_{\text{tav}}/N^2$ depend

on the initial value and disappear in the ensemble average. We have also checked that the short time mean field behavior approaches the correct quantum dynamics for larger N .

We can now explore the role of dissipation for the formation of the time crystal. In Fig. 2(b) we switch off dissipation by hand, setting $V_1 = 0$ and show the trajectory of $X(t) = \varphi_\uparrow^*\varphi_\downarrow + \varphi_\downarrow^*\varphi_\uparrow$, $Y(t) = i(\varphi_\downarrow^*\varphi_\uparrow - \varphi_\uparrow^*\varphi_\downarrow)$, $Z(t) = |\varphi_\uparrow|^2 - |\varphi_\downarrow|^2$ with $V_1 \neq 0$ (black) and $V_1 = 0$ (red) and after times $\omega t > 1.1 \times 10^3$ where we have reached the stationary state. Note that $X^2 + Y^2 + Z^2 = N^2$ is a conserved quantity such that trajectories lie always on a sphere. The black curve shows a limit cycle, a stable oscillation on the sphere. In contrast, the red curve shows a highly oscillatory behavior. This key finding demonstrates the role of dissipation and that it can be described as a cooling mechanism for the atoms which stabilizes the dissipative time crystal.

Threshold to dynamical Superradiance— Last but not least it is possible to derive analytical results for the onset of superradiance using Floquet theory. We assume that all atoms are initially in the ground state and explore when driving induces an instability towards superradiance. With most bosons in $|\downarrow\rangle$, we eliminate fluctuations in the ground state using $\varphi_\downarrow \approx \sqrt{N}$, which linearizes Eq. (8). The resulting complex differential equation for $\varphi_\uparrow = (\varphi_\uparrow, \varphi_\uparrow^*)$ can be solved using Floquet theory by making the ansatz $\varphi_\uparrow(t) = e^{\lambda_{\text{F1}}t}\mathbf{u}(t)$ with a $T = 2\pi/\omega$ periodic vector \mathbf{u} and the Floquet eigenvalue $\lambda_{\text{F1}} = \gamma_{\text{F1}} - i\nu_{\text{F1}}$, $\gamma_{\text{F1}}, \nu_{\text{F1}} \in \mathbb{R}$. Details of this derivation are reported in the appendix. The stability of the fluctuations is determined by γ_{max} which is the maximum of all possible real parts γ_{F1} . Whenever $\gamma_{\text{max}} \leq 0$ ($\gamma_{\text{max}} > 0$) we expect the system to be non-superradiant (superradiant). The boundary to superradiance that is calculated with this method is shown as black line in Fig. 1 and predicts accurately the superradiant regions. Furthermore, to get analytical insight, we reformulate the coupled complex differential equation as real second-order differential equation for $x_\uparrow = \varphi_\uparrow + \varphi_\uparrow^*$

$$\frac{d^2x_\uparrow}{dt^2} + 2V_1(t)\frac{dx_\uparrow}{dt} + \Delta[\Delta - 2V_0(t)]x_\uparrow = 0. \quad (9)$$

In this differential equation V_0 modifies the resonance frequency Δ originating from the (i) cavity-mediated interactions and V_1 serves as a damping of fluctuations coming from (ii) the cavity-generated dissipation. If we perform a first order perturbation theory in $g_1/g_0 \sim \Delta/\sqrt{\delta_c^2 + \kappa^2}$, Eq. (9) becomes a Mathieu equation [32] with $V_1(t) \approx \gamma_0$ and $\Delta[\Delta - 2V_0(t)] \approx \omega_{\text{res}}^2 - 8\Delta\delta_c g_0 g_1/[\delta_c^2 + \kappa^2] \cos(\omega t)$. Here, we have introduced the time-independent damping

$$\gamma_0 = \frac{4\kappa\delta_c\Delta g_0^2}{[\delta_c^2 + \kappa^2]^2}, \quad (10)$$

and resonance frequency

$$\omega_{\text{res}} = \Delta \sqrt{1 - \frac{g^2}{g_c^2}}. \quad (11)$$

The Mathieu equation without damping is known to exhibit instabilities around the parametric resonances $n\omega = 2\omega_{\text{res}}$ [32]. In presence of damping γ_0 , instabilities require sufficiently strong driving, provided by the time-periodic term [32]. Accordingly we observe in Fig 1 superradiance close to the resonance condition $n\omega = 2\omega_{\text{res}}$ for pump power in the sidebands $\propto g_1/g_0$ above a certain threshold. This finding is in agreement with previous works where dynamical superradiance has been connected to the Mathieu equation [14, 23], which again shows that the atomic quantum theory in Eq. (5) gives the correct behavior without describing explicitly the cavity. Moreover, this allows us to obtain simple results for the damping rate (10) and resonance frequency (11) and enables us to calculate the threshold in g_1 . For this we perform a perturbative analysis around the first instability at $\omega = 2\omega_{\text{res}}$ reported in the appendix. We show that the instability occurs at

$$g_1^c = \frac{2\kappa\omega_{\text{res}}g_0}{\delta_c^2 + \kappa^2}. \quad (12)$$

The result given by Eq. (12) is visible as gray solid line in Fig. 1. It agrees well with the threshold found using Floquet theory at $\omega = 2\omega_{\text{res}}$ and highlights the role of dissipation in determining the threshold.

Dynamical response of the atoms— For a more comprehensive test of the atom-only theory and the resulting Floquet theory, we again turn to semiclassical simulations of atoms and cavity (see appendix) for the same parameters as in Fig. 1, $g_1 = 0.75g_0$, and different values of ω (black dashed line in Fig. 1). For these parameters we expect three superradiant regimes around the parametric resonance $\omega = 2\omega_{\text{res}}$, $2\omega = 2\omega_{\text{res}}$, and $3\omega = 2\omega_{\text{res}}$. We use the semiclassical simulations to calculate $\langle \hat{X}^2(t) \rangle$ shown as function of time t and driving frequency ω in Fig. 3(a). The atom only theory predicts the borders of the superradiant regimes (black vertical lines), which fully agrees with large values $\langle \hat{X}^2 \rangle \propto N^2$. In Fig. 3(b), to compare the stationary state, we show the time-averaged superradiant order parameter $\langle \hat{X}^2 \rangle_{\text{tav}}$ for both, the semiclassical simulation of atoms and field (circles) and the atom-only mean-field theory (black solid line) at steady state. Both show a remarkable asymmetry of $\langle \hat{X}^2 \rangle_{\text{tav}}$ where at each resonance the lower threshold to superradiance is a continuous transition while the upper threshold is marked by a sudden jump of $\langle \hat{X}^2 \rangle_{\text{tav}}$. In general, we find excellent agreement between the mean-field and semiclassical results which shows that the atom-only theory predicts the correct stationary state in a large parameter space.

To understand the dynamical response of the atoms, which is crucial to determine whether one finds a subharmonic and time-crystalline order, we employ the two-time

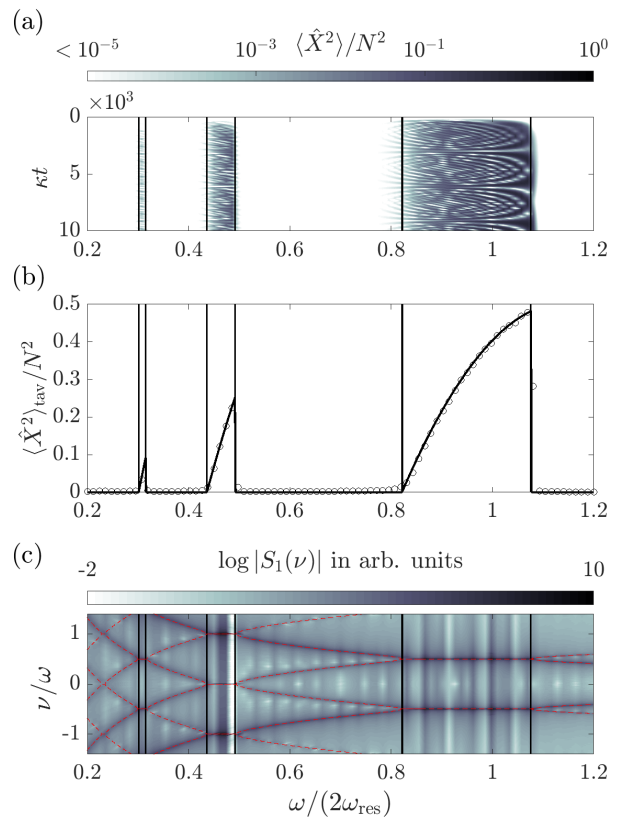


FIG. 3. (a) Superradiant order parameter $\langle \hat{X}^2 \rangle$ obtained from stochastic simulations as function of time in units of $1/\kappa$ and of $\omega/(2\omega_{\text{res}})$. The vertical black solid lines mark the threshold of superradiance obtained from the atom-only stability analysis. (b) Time-averaged superradiant order parameter $\langle \hat{X}^2 \rangle_{\text{tav}}$ as function of $\omega/(2\omega_{\text{res}})$ evaluated after a time $\kappa t = 10^4$ where the atoms have reached steady state. The solid black lines are obtained from the mean-field equations and the circles from the semiclassical simulations. (c) Spectrum $S_1(\nu)$ calculated from the stochastic simulations with $\kappa t_0 = 5 \times 10^3$ and where we choose $t_{\text{max}} = t_0$. The spectrum is shown as function of ν/ω and $\omega/(2\omega_{\text{res}})$. The red dashed lines in (c) show the imaginary part ν_{FI} of the Floquet spectrum. Remaining parameters are $\delta_c = \kappa$, $\Delta = 0.1\kappa$, $g_0 = 0.5g_c$. The stochastic simulations are averaged over 10^4 trajectories.

correlation function $g_1(t, t_0) = \langle \hat{X}(t + t_0)\hat{X}(t_0) \rangle$ and calculate its Fourier transform $S_1(\nu) = \int_0^{t_{\text{max}}} dt e^{i\nu t} g_1(t, t_0)$. Here, t_0 is a long time after which the dynamics of the system becomes independent of its initial condition and t_{max} is a long-time cut-off. The numerical result of $S_1(\nu)$ is shown in Fig. 3(c) as function of ν and driving frequency ω . The spectrum $S_1(\nu)$ spikes in ν for all values of ω that highlight resonances in the atomic medium. These resonances are in agreement with the Floquet frequencies ν_{FI} that are visible as red dashed lines in Fig. 3(c). We find $\nu_{\text{FI}} = n\omega/2$ in the dynamical superradiant phase

corresponding to the parametric resonance $n\omega = 2\omega_{\text{res}}$. This implies that the response of the atoms is flat with respect to the driving frequency which leads to an inherit robustness. Moreover, the response is subharmonic whenever n is odd which becomes clear when considering that the underlying model is a single-mode theory of \hat{b}_\uparrow that oscillate with ω_{res} : the first resonance at $\omega = 2\omega_{\text{res}}$ describes resonant excitation of bosons with frequency $\omega_{\text{res}} = \omega/2$, the second resonance $2\omega = 2\omega_{\text{res}}$ would result in a response with the same periodicity $\omega_{\text{res}} = \omega$ and so on.

Conclusions—In conclusion, we have derived and verified an atom-only theory for the time-periodic dissipative Dicke model. With this theory we studied the onset of superradiance including the dynamical response and the threshold determined by the cavity-generated dissipation, the driving frequency and amplitude. Besides the numerical efficiency and maybe most remarkably, this atom-only theory allows us also to describe the long-time relaxation into a dissipative time crystalline structure that we can understand from an effective cooling mechanism. We remark that all studied quantities in this paper including the superradiance order parameter and spectrum can be measured from the cavity output. This is a consequence of working in the regime where the cavity adiabatically follows the atomic motion which enables to make detailed experimental predictions for the cavity field intensity and spectrum based on an atom-only description. Future theoretical avenues that build on the presented theory could use the atom-only theory to derive quantum fluctuations and low energy excitations of the dissipative time crystal. This can be used to determine if the emergent states are quantum entangled [33]. In addition, one can apply the atom-only theory to more complicated systems with many and eventually infinitely many atomic modes. This paves the way to the efficient theoretical description of the atomic medium under periodic driving, which can be used to analyze the generation of squeezed and entangled atomic states with quantum information and metrology applications.

SBJ acknowledges stimulating discussions with A. Pelster, R. Betzholz, G. Morigi, J. Reilly, and M. J. Holland. We acknowledge support from Research Centers of the Deutsche Forschungsgemeinschaft (DFG): Projects A4 and A5 in SFB/Transregio 185: OSCAR.

APPENDIX

Elimination of the cavity field

In this section we present details on the derivation of the operator $\hat{\beta}$ which is determined by

$$i\frac{\partial\hat{\beta}}{\partial t} = (\delta_c - i\kappa)\hat{\beta} + \frac{g(t)}{\sqrt{N}} \left(\hat{b}_\uparrow^\dagger \hat{b}_\downarrow + \hat{b}_\downarrow^\dagger \hat{b}_\uparrow \right) + [\Delta\hat{n}_\uparrow, \hat{\beta}]. \quad (13)$$

To solve this equation we make the ansatz $\hat{\beta}(t) = c_+(t)\hat{b}_\uparrow^\dagger\hat{b}_\downarrow + c_-(t)\hat{b}_\downarrow^\dagger\hat{b}_\uparrow$ which results in the following equations

$$i\frac{dc_\pm}{dt} = (\delta_c \pm \Delta - i\kappa)c_\pm + \frac{g(t)}{\sqrt{N}}. \quad (14)$$

and can be formally solved

$$c_\pm \approx \frac{-i}{\sqrt{N}} \int_0^t d\tau e^{[-i(\delta_c \pm \Delta) - \kappa]\tau} g(t - \tau) \quad (15)$$

where we dropped the homogeneous solution since it is negligible after times $t \gg \kappa^{-1}$. Assuming $\omega \ll \kappa, \delta_c$ we can use that $g(t)$ changes sufficiently slow such that we can approximate in the integral $g(t - \tau) = g(t) - \tau\dot{g}(t)$ and arrive at

$$\begin{aligned} c_\pm &\approx -\frac{g(t)}{\sqrt{N}[\delta_c \pm \Delta - i\kappa]} - \frac{i\dot{g}(t)}{\sqrt{N}[(\delta_c \pm \Delta) - i\kappa]^2} \\ &\approx -\frac{1}{\sqrt{N}} \left(\frac{g(t)}{\delta_c - i\kappa} + \frac{i\dot{g}(t)}{[\delta_c - i\kappa]^2} \mp \frac{\Delta g(t)}{[\delta_c - i\kappa]^2} \right) \end{aligned} \quad (16)$$

where we used $\kappa t \gg 1$ for the first equation and $\Delta, \omega \ll \delta_c, \kappa$ in the second equation. This shows the result presented in the Letter.

Derivation of the mean-field equations

In this section we derive the mean-field equations that are presented in the main text from the master equation

$$\frac{\partial\hat{\rho}_{\text{at}}}{\partial t} = -i \left[\hat{H}_{\text{at}}, \hat{\rho}_{\text{at}} \right] - \kappa (\hat{\beta}^\dagger \hat{\beta} \hat{\rho}_{\text{at}} + \hat{\rho}_{\text{at}} \hat{\beta}^\dagger \hat{\beta} - 2\hat{\beta} \hat{\rho}_{\text{at}} \hat{\beta}^\dagger). \quad (17)$$

To do this we derive the differential equations $\varphi_s = \langle \hat{b}_s \rangle$ for $s = \uparrow, \downarrow$. We use

$$\frac{d\langle \hat{b}_s \rangle}{dt} = -i \left[\hat{b}_s, \hat{H}_{\text{at}} \right] - \kappa \left\langle \hat{\beta}^\dagger [\hat{\beta}, \hat{b}_s] + [\hat{b}_s, \hat{\beta}^\dagger] \hat{\beta} \right\rangle \quad (18)$$

and $\hat{\beta}(t) = c_+(t)\hat{b}_\uparrow^\dagger\hat{b}_\downarrow + c_-(t)\hat{b}_\downarrow^\dagger\hat{b}_\uparrow$ to find

$$\begin{aligned} \frac{d\varphi_\downarrow}{dt} &= -i\frac{g(t)}{\sqrt{N}}\text{Re}(c_+ + c_-)|\varphi_\uparrow|^2\varphi_\downarrow \\ &\quad - i\frac{g(t)}{\sqrt{N}}(c_+^* + c_-)(\varphi_\uparrow)^2\varphi_\downarrow^* \\ &\quad + \kappa(|c_-|^2 - |c_+|^2)|\varphi_\uparrow|^2\varphi_\downarrow, \end{aligned} \quad (19)$$

$$\begin{aligned} \frac{d\varphi_\uparrow}{dt} &= -i\Delta\varphi_\uparrow - i\frac{g(t)}{\sqrt{N}}\text{Re}(c_+ + c_-)|\varphi_\downarrow|^2\varphi_\uparrow \\ &\quad - i\frac{g(t)}{\sqrt{N}}(c_+ + c_-^*)(\varphi_\downarrow)^2\varphi_\uparrow^* \\ &\quad + \kappa(|c_+|^2 - |c_-|^2)|\varphi_\downarrow|^2\varphi_\uparrow. \end{aligned} \quad (20)$$

To derive these equations we have made a mean-field approximation where we can factorize the expectation value of arbitrary products of annihilation and creation operators.

Using Eq. (16) we can then derive

$$\frac{g(t)}{\sqrt{N}}\text{Re}(c_+ + c_-) = -\frac{V_0}{N} \quad (21)$$

$$\frac{g(t)}{\sqrt{N}}(c_+^* + c_-) = -\frac{V_0 + iV_1}{N} \quad (22)$$

$$\kappa(|c_-|^2 - |c_+|^2) = \frac{V_1}{N} \quad (23)$$

with

$$V_0 = \frac{2\delta_c g^2(t)}{\delta_c^2 + \kappa^2} - \frac{4\delta_c \kappa g(t)\dot{g}(t)}{[\delta_c^2 + \kappa^2]^2}, \quad (24)$$

$$V_1 = \frac{4\delta_c \Delta \kappa g^2(t)}{[\delta_c^2 + \kappa^2]^2}. \quad (25)$$

Inserting the above equations in Eqs. (19) and (20) leads to the mean-field description shown in the main text.

Dynamics in the $|\varphi_\uparrow| \ll \sqrt{N}$ approximation

In this section we present a special case of the mean-field equations using the approximations $|\varphi_\uparrow| \ll \sqrt{N}$ and $|\varphi_\downarrow| \approx \sqrt{N}$. From these equations we also show how one can derive the second order differential equation that is given in the Letter.

Using $\varphi_\downarrow \approx \sqrt{N}$ we can derive a complex differential equation for φ_\uparrow which reads

$$\frac{d\varphi_\uparrow}{dt} = -i[\Delta - (V_0 + iV_1)]\varphi_\uparrow + i(V_0 - iV_1)\varphi_\uparrow^*. \quad (26)$$

This differential equation together with its complex conjugate can be given as a non-hermitian Schrödinger equation

$$\frac{d\varphi_\uparrow}{dt} = -i\Upsilon\mathbf{H}_{\text{nh}}\varphi_\uparrow. \quad (27)$$

with $\varphi_\uparrow = (\varphi_\uparrow, \varphi_\uparrow^*)^T$, the diagonal matrix $\Upsilon = \text{diag}(1, -1)$ and the non-hermitian Hamiltonian

$$\mathbf{H}_{\text{nh}} = \begin{pmatrix} \Delta - V_0 - iV_1 & -V_0 + iV_1 \\ -V_0 - iV_1 & \Delta - V_0 + iV_1 \end{pmatrix}. \quad (28)$$

In a next step we derive from Eq. (27) the second order differential equation that is presented in the main text. For this we define $x_\uparrow = \varphi_\uparrow + \varphi_\uparrow^*$ and $y_\uparrow = i(\varphi_\uparrow - \varphi_\uparrow^*)$ and derive

$$\frac{dx_\uparrow}{dt} = -\Delta y_\uparrow, \quad (29)$$

$$\frac{dy_\uparrow}{dt} = (\Delta - 2V_0)x_\uparrow - 2V_1 y_\uparrow. \quad (30)$$

Taking the derivative of Eq. (29) and inserting Eq. (30) we arrive at the second order differential equation that was presented in the main text.

Details of the Floquet analysis

In this section we present details on the Floquet analysis presented in the paper. We use Floquet theory for the linear differential equation (27) with $g = g_0 + g_1 \cos(\omega t)$ and decompose its square into Fourier components, $g^2(t) = g_0^2 + 2g_0 g_1 \cos(\omega t) + g_1^2 \cos^2(\omega t)$. Accordingly, we decompose the linear operator $\mathbf{A}(t) = -i\Upsilon\mathbf{H}_{\text{nh}}(t)$ into Fourier components

$$\mathbf{A}(t) = \sum_{m=-2}^2 \mathbf{A}^{(m)} e^{-im\omega t} \quad (31)$$

with

$$\mathbf{A}^{(0)} = \begin{pmatrix} -i(\omega_0 - V_0^{(0)}) - V_1^{(0)} & iV_0^{(0)} + V_1^{(0)} \\ -iV_0^{(0)} + V_1^{(0)} & i(\omega_0 - V_0^{(0)}) - V_1^{(0)} \end{pmatrix} \quad (32)$$

and

$$V_0^{(0)} = \frac{2\delta_c \left[g_0^2 + \frac{g_1^2}{2} \right]}{\delta_c^2 + \kappa^2}, \quad (33)$$

$$V_1^{(0)} = \frac{4\kappa\delta_c\omega_0 \left[g_0^2 + \frac{g_1^2}{2} \right]}{[\delta_c^2 + \kappa^2]^2}. \quad (34)$$

The rotating components with ω are given by

$$\mathbf{A}^{(\pm 1)} = \begin{pmatrix} iV_0^{(\pm 1)} - V_1^{(\pm 1)} & iV_0^{(\pm 1)} + V_1^{(\pm 1)} \\ -iV_0^{(\pm 1)} + V_1^{(\pm 1)} & -iV_0^{(\pm 1)} - V_1^{(\pm 1)} \end{pmatrix}, \quad (35)$$

and

$$V_0^{(\pm 1)} = \frac{2\delta_c g_0 g_1}{\delta_c^2 + \kappa^2} \mp \frac{i2\delta_c \kappa \omega g_0 g_1}{[\delta_c^2 + \kappa^2]^2}, \quad (36)$$

$$V_1^{(\pm 1)} = \frac{4\kappa\delta_c\omega_0 g_0 g_1}{[\delta_c^2 + \kappa^2]^2}. \quad (37)$$

The next order, rotating with 2ω , are given by

$$\mathbf{A}^{(\pm 2)} = \begin{pmatrix} iV_0^{(\pm 2)} - V_1^{(\pm 2)} & iV_0^{(\pm 2)} + V_1^{(\pm 2)} \\ -iV_0^{(\pm 2)} + V_1^{(\pm 2)} & -iV_0^{(\pm 2)} - V_1^{(\pm 2)} \end{pmatrix}, \quad (38)$$

where we defined

$$V_0^{(\pm 2)} = \frac{2\delta_c \frac{g_1^2}{4}}{\delta_c^2 + \kappa^2} \mp \frac{i4\delta_c \kappa \omega \frac{g_1^2}{4}}{[\delta_c^2 + \kappa^2]^2}, \quad (39)$$

$$V_1^{(\pm 2)} = \frac{4\kappa\delta_c\omega_0 \frac{g_1^2}{4}}{[\delta_c^2 + \kappa^2]^2}. \quad (40)$$

We apply now Floquet theory to the liner system

$$\frac{d\mathbf{v}}{dt} = \mathbf{A}\mathbf{v}. \quad (41)$$

For this we write $\boldsymbol{\varphi}_\uparrow(t) = e^{\lambda t}\mathbf{u}(t)$ with a time-periodic $\mathbf{u}(t) = \mathbf{u}(t+T)$ and $T = 2\pi/\omega$. We find then

$$\lambda\mathbf{u} + \frac{d\mathbf{u}}{dt} = \mathbf{A}\mathbf{u}. \quad (42)$$

Since \mathbf{u} is periodic with period T , we can decompose it into Fourier components

$$\mathbf{u} = \sum_n \mathbf{u}_n e^{in\omega t} \quad (43)$$

and find

$$\lambda\mathbf{u}_n = \sum_{m=-2}^2 [\mathbf{A}^{(m)} - in\delta_{m,0}\omega]\mathbf{u}_{n-m}. \quad (44)$$

Defining now the 2×2 identity matrix \mathbf{I}_2 we can find the solution of the above equation by finding the eigenvalues λ_{FI} and eigenvectors

$$\mathbf{u} = \sum_{n=-\infty}^{\infty} \mathbf{u}_n \otimes |n\rangle \quad (45)$$

of

$$\mathbf{A} = \sum_{n=-\infty}^{\infty} \sum_{m=-2}^2 [\mathbf{A}^{(m)} - in\omega\delta_{m,0}\mathbf{I}_2] |n\rangle\langle n-m|. \quad (46)$$

The latter is approximated using a sufficiently high cut-off in n such that the results have converged.

Threshold for $\omega = 2\omega_{\text{res}}$

In this section we derive the estimate for the critical value g_1^c close to resonance $\omega = 2\omega_{\text{res}} + \epsilon$, $\epsilon \ll \omega_{\text{res}}$, using perturbation theory. This is done in the limit where $g_1 \ll g_0$ where we can use the Mathieu equation

$$\frac{d^2 x_\uparrow}{dt^2} + 2\gamma_0 \frac{dx_\uparrow}{dt} + [\omega_{\text{res}}^2 - 4\Delta b \cos(\omega t)] x_\uparrow = 0 \quad (47)$$

with $b = 2\delta_c g_0 g_1 / (\delta_c^2 + \kappa^2)$. Equivalent derivations of the threshold are given in Ref. [32, 34]. We assume that $\gamma_0, \sqrt{\Delta b} \ll \omega_{\text{res}}$ and make the ansatz

$$x_\uparrow = \sum_{n=-\infty}^{\infty} x_n(t) e^{-i\frac{n\omega}{2}t}. \quad (48)$$

The functions x_n are time-dependent Fourier amplitudes. We can then derive a differential equation for x_n that takes the form

$$\begin{aligned} \ddot{x}_n - (in\omega - 2\gamma_0)\dot{x}_n - \left[\left(\frac{n^2\omega^2}{4} - \omega_{\text{res}}^2 \right) + in\gamma_0\omega \right] x_n \\ = 2\Delta b(x_{n-2} + x_{n+2}) \end{aligned} \quad (49)$$

From the equation above we observe that all amplitudes x_n with $n^2 \neq 1$ are of higher order in $2\Delta b/\omega_{\text{res}}^2$. Thus we restrict the equations of motion to $n = \pm 1$. The components $x_{\pm 1}$ are evolving slowly with $\dot{x}_{\pm 1}/x_{\pm 1} \ll \omega_{\text{res}}$. In this regime we can approximate the differential equation by

$$\frac{d}{dt} \begin{pmatrix} x_1 \\ x_{-1} \end{pmatrix} = \mathbf{A} \begin{pmatrix} x_1 \\ x_{-1} \end{pmatrix} \quad (50)$$

with

$$\mathbf{A} = \begin{pmatrix} -\gamma_0 + i\frac{\epsilon}{2} & i\frac{\Delta b}{\omega_{\text{res}}} \\ -i\frac{\Delta b}{\omega_{\text{res}}} & -\gamma_0 - i\frac{\epsilon}{2} \end{pmatrix}, \quad (51)$$

where we used $\omega^2 \approx 4\omega_{\text{res}}(\omega_{\text{res}} + \epsilon)$. The eigenfrequencies are given by the eigenvalues of \mathbf{A} and to derive them we calculate the characteristic polynomial

$$p(\lambda) = \det[\mathbf{A} - \lambda\mathbf{I}_2] = (\lambda + \gamma_0)^2 + \frac{\epsilon^2}{4} - \frac{\Delta^2 b^2}{\omega_{\text{res}}^2}. \quad (52)$$

The zeros of this polynomial are the eigenfrequencies that are given by

$$\lambda_{\pm} = -\gamma_0 \pm \sqrt{\frac{\Delta^2 b^2}{\omega_{\text{res}}^2} - \frac{\epsilon^2}{4}}. \quad (53)$$

The fluctuations are stable if the solution is damped. This is the case if

$$g_1^2 \leq \frac{4\kappa^2\omega_{\text{res}}^2 g_0^2}{(\delta_c^2 + \kappa^2)^2} + \frac{(\delta_c^2 + \kappa^2)^2 \omega_{\text{res}}^4}{4\delta_c^2 \Delta^2 g_0^2} \left(1 - \frac{\omega}{2\omega_{\text{res}}} \right)^2. \quad (54)$$

Therefore, at resonance $\omega = 2\omega_{\text{res}}$, we find the threshold which is given in the main text.

Stochastic Simulation of the dissipative Dicke model

In this section we give the explicit form of the stochastic differential equation that we integrate to find part of

the numerical results given in the main text. We define the operators

$$\hat{X} = \hat{b}_\uparrow^\dagger \hat{b}_\downarrow + \hat{b}_\downarrow^\dagger \hat{b}_\uparrow \quad (55)$$

$$\hat{Y} = i(\hat{b}_\uparrow^\dagger \hat{b}_\uparrow - \hat{b}_\downarrow^\dagger \hat{b}_\downarrow) \quad (56)$$

$$\hat{Z} = \hat{b}_\uparrow^\dagger \hat{b}_\uparrow - \hat{b}_\downarrow^\dagger \hat{b}_\downarrow. \quad (57)$$

Our starting point are the Heisenberg-Langevin equations for these operators and cavity degrees of freedom

$$\frac{d\hat{a}}{dt} = -\kappa\hat{a} - i\delta_c\hat{a} - i\frac{g}{\sqrt{N}}\hat{X} + \sqrt{2\kappa}\hat{a}_{\text{in}}(t), \quad (58)$$

$$\frac{d\hat{X}}{dt} = -\Delta\hat{Y}, \quad (59)$$

$$\frac{d\hat{Y}}{dt} = \Delta\hat{X} - 2\frac{g(t)}{\sqrt{N}}(\hat{a} + \hat{a}^\dagger)\hat{Z}, \quad (60)$$

$$\frac{d\hat{Z}}{dt} = 2\frac{g(t)}{\sqrt{N}}(\hat{a} + \hat{a}^\dagger)\hat{Y}. \quad (61)$$

We introduced the noise operators \hat{a}_{in} with vanishing mean value $\langle \hat{a}_{\text{in}} \rangle = 0$, second moments $\langle \hat{a}_{\text{in}}(t)\hat{a}_{\text{in}}(t') \rangle = 0 = \langle \hat{a}_{\text{in}}^\dagger(t)\hat{a}_{\text{in}}(t') \rangle$ and $\langle \hat{a}_{\text{in}}(t)\hat{a}_{\text{in}}^\dagger(t') \rangle = \delta(t-t')$.

Instead of evolving the complex field we define the hermitian quadratures $\hat{a}_x = \hat{a}^\dagger + \hat{a}$ and $\hat{a}_p = i(\hat{a}^\dagger - \hat{a})$. Their time evolution coupled to the spin degrees is given by

$$\frac{d\hat{a}_x}{dt} = -\kappa\hat{a}_x + \delta_c\hat{a}_p + \sqrt{2\kappa}\hat{\mathcal{N}}^x(t), \quad (62)$$

$$\frac{d\hat{a}_p}{dt} = -\kappa\hat{a}_p - \delta_c\hat{a}_x - 2\frac{g(t)}{\sqrt{N}}\hat{X} + \sqrt{2\kappa}\hat{\mathcal{N}}^p(t), \quad (63)$$

$$\frac{d\hat{X}}{dt} = -\Delta\hat{Y}, \quad (64)$$

$$\frac{d\hat{Y}}{dt} = \Delta\hat{X} - 2\frac{g(t)}{\sqrt{N}}\hat{a}_x\hat{Z}, \quad (65)$$

$$\frac{d\hat{Z}}{dt} = 2\frac{g(t)}{\sqrt{N}}\hat{a}_x\hat{Y}, \quad (66)$$

with $\hat{\mathcal{N}}^x = [\hat{a}_{\text{in}}(t) + \hat{a}_{\text{in}}^\dagger(t)]$ and $\hat{\mathcal{N}}^p = -i[\hat{a}_{\text{in}}(t) - \hat{a}_{\text{in}}^\dagger(t)]$. The stochastic differential equations that are used in the main part of the paper are now derived by exchanging the quantum operators with real functions using a symmetric ordering. In addition we exchange the quantum noise by classical noise which warrants the correct second moments [35]. The stochastic semiclassical differential equations are

$$\frac{da_x}{dt} = -\kappa a_x + \delta_c a_p + \sqrt{2\kappa}\mathcal{N}^x(t), \quad (67)$$

$$\frac{da_p}{dt} = -\kappa a_p - \delta_c a_x - 2\frac{g}{\sqrt{N}}X + \sqrt{2\kappa}\mathcal{N}^p(t), \quad (68)$$

$$\frac{dX}{dt} = -\Delta Y, \quad (69)$$

$$\frac{dY}{dt} = \Delta X - 2\frac{g}{\sqrt{N}}a_x Z, \quad (70)$$

$$\frac{dZ}{dt} = 2\frac{g}{\sqrt{N}}a_x Y, \quad (71)$$

with \mathcal{N}^a fulfilling $\langle \mathcal{N}^a \rangle = 0$ and $\langle \mathcal{N}^a(t)\mathcal{N}^b(t') \rangle = \delta_{ab}\delta(t-t')$. We use these stochastic differential equations to simulate the semiclassical dynamics of the coupled spin and cavity dynamics. In this paper we consider as the initial state with $\langle Z \rangle = -N$, $\langle X \rangle = 0 = \langle Y \rangle$ and the cavity in the vacuum state $\langle a_x \rangle = \langle a_p \rangle = 0$. To incorporate quantum fluctuations in the stochastic semiclassical variables a_x , a_p , X , Y , and Z , we initialize them by independent Gaussian random variables with $\langle a_x^2 \rangle = 1 = \langle a_p^2 \rangle$, $\langle X^2 \rangle = N = \langle Y^2 \rangle$, and $\langle Z^2 \rangle = \langle Z \rangle^2 = N^2$. With these initial conditions we integrate the stochastic differential equations and average over several initializations that we report in the captions of the figures in the main text.

-
- [1] J. Dalibard, F. Gerbier, G. Juzeliūnas, and P. Öhberg, Colloquium: Artificial gauge potentials for neutral atoms, *Rev. Mod. Phys.* **83**, 1523 (2011).
 - [2] K. Wintersperger, C. Braun, F. N. Ünal, A. Eckardt, M. D. Liberto, N. Goldman, I. Bloch, and M. Aidelsburger, Realization of an anomalous floquet topological system with ultracold atoms, *Nature Physics* **16**, 1058 (2020).
 - [3] K. Staliunas, S. Longhi, and G. J. de Valcárcel, Faraday patterns in bose-einstein condensates, *Phys. Rev. Lett.* **89**, 210406 (2002).
 - [4] C. Chin, R. Grimm, P. Julienne, and E. Tiesinga, Feshbach resonances in ultracold gases, *Rev. Mod. Phys.* **82**, 1225 (2010).
 - [5] A. M. Perego, N. Tarasov, D. V. Churkin, S. K. Turitsyn, and K. Staliunas, Pattern generation by dissipative parametric instability, *Phys. Rev. Lett.* **116**, 028701 (2016).
 - [6] L. W. Clark, A. Gaj, L. Feng, and C. Chin, Collective emission of matter-wave jets from driven bose-einstein condensates, *Nature* **551**, 356 (2017).
 - [7] J. H. V. Nguyen, M. C. Tsatsos, D. Luo, A. U. J. Lode, G. D. Telles, V. S. Bagnato, and R. G. Hulet, Parametric excitation of a bose-einstein condensate: From faraday waves to granulation, *Phys. Rev. X* **9**, 011052 (2019).
 - [8] Z. Zhang, K.-X. Yao, L. Feng, J. Hu, and C. Chin, Pattern formation in a driven bose-einstein condensate, *Nature Physics* **16**, 652 (2020).
 - [9] S. Fazzini, P. Chudzinski, C. Dauer, I. Schneider, and S. Eggert, Nonequilibrium floquet steady states of time-periodic driven luttinger liquids, *Phys. Rev. Lett.* **126**, 243401 (2021).
 - [10] A. Eckardt, Colloquium: Atomic quantum gases in periodically driven optical lattices, *Rev. Mod. Phys.* **89**, 011004 (2017).
 - [11] C. Weitenberg and J. Simonet, Tailoring quantum gases by floquet engineering, *Nature Physics* **17**, 1342 (2021).
 - [12] F. Petziol and A. Eckardt, Cavity-based reservoir engineering for floquet-engineered superconducting circuits, *Phys. Rev. Lett.* **129**, 233601 (2022).
 - [13] B. Zhu, J. Marino, N. Y. Yao, M. D. Lukin, and E. A. Demler, Dicke time crystals in driven-dissipative quantum many-body systems, *New J. Phys.* **21**, 073028 (2019).

- [14] R. Chitra and O. Zilberberg, Dynamical many-body phases of the parametrically driven, dissipative dicke model, *Phys. Rev. A* **92**, 023815 (2015).
- [15] F. Iemini, A. Russomanno, J. Keeling, M. Schirò, M. Dalmonte, and R. Fazio, Boundary Time Crystals, *Phys. Rev. Lett.* **121**, 035301 (2018).
- [16] Z. Gong, R. Hamazaki, and M. Ueda, Discrete Time-Crystalline Order in Cavity and Circuit QED Systems, *Phys. Rev. Lett.* **120**, 040404 (2018).
- [17] H. Keßler, P. Kongkhambut, C. Georges, L. Mathey, J. G. Cosme, and A. Hemmerich, Observation of a dissipative time crystal, *Phys. Rev. Lett.* **127**, 043602 (2021).
- [18] P. Kongkhambut, H. Keßler, J. Skulte, L. Mathey, J. G. Cosme, and A. Hemmerich, Realization of a periodically driven open three-level dicke model, *Phys. Rev. Lett.* **127**, 253601 (2021).
- [19] P. Kongkhambut, J. Skulte, L. Mathey, J. G. Cosme, A. Hemmerich, and H. K. ler, Observation of a continuous time crystal, *Science* **377**, 670 (2022).
- [20] H. Ritsch, P. Domokos, F. Brennecke, and T. Esslinger, Cold atoms in cavity-generated dynamical optical potentials, *Rev. Mod. Phys.* **85**, 553 (2013).
- [21] F. Mivehvar, F. Piazza, T. Donner, and H. Ritsch, Cavity qed with quantum gases: new paradigms in many-body physics, *Adv. Phys.* **70**, 1 (2021).
- [22] N. Defenu, T. Donner, T. Macri, G. Pagano, S. Ruffo, and A. Trombettoni, Long-range interacting quantum systems, arXiv:2109.01063 (2021), 2109.01063.
- [23] P. Mognini, L. Papariello, A. U. J. Lode, and R. Chitra, Superlattice switching from parametric instabilities in a driven-dissipative bose-einstein condensate in a cavity, *Phys. Rev. A* **98**, 053620 (2018).
- [24] J. G. Cosme, J. Skulte, and L. Mathey, Time crystals in a shaken atom-cavity system, *Phys. Rev. A* **100**, 053615 (2019).
- [25] F. Damanet, A. J. Daley, and J. Keeling, Atom-only descriptions of the driven-dissipative Dicke model, *Phys. Rev. A* **99**, 033845 (2019).
- [26] A. V. Bezvershenko, C.-M. Halati, A. Sheikhan, C. Kollath, and A. Rosch, Dicke Transition in Open Many-Body Systems Determined by Fluctuation Effects, *Phys. Rev. Lett.* **127**, 173606 (2021).
- [27] S. B. Jäger, T. Schmit, G. Morigi, M. J. Holland, and R. Betzholz, Lindblad master equations for quantum systems coupled to dissipative bosonic modes, *Phys. Rev. Lett.* **129**, 063601 (2022).
- [28] F. Dimer, B. Estienne, A. S. Parkins, and H. J. Carmichael, Proposed realization of the Dicke-model quantum phase transition in an optical cavity QED system, *Phys. Rev. A* **75**, 013804 (2007).
- [29] K. Baumann, C. Guerlin, F. Brennecke, and T. Esslinger, Dicke quantum phase transition with a superfluid gas in an optical cavity, *Nature* **464**, 1301 (2010).
- [30] E. G. Dalla Torre, S. Diehl, M. D. Lukin, S. Sachdev, and P. Strack, Keldysh approach for nonequilibrium phase transitions in quantum optics: Beyond the Dicke model in optical cavities, *Phys. Rev. A* **87**, 023831 (2013).
- [31] P. Kirton, M. M. Roses, J. Keeling, and E. G. Dalla Torre, Introduction to the dicke model: From equilibrium to nonequilibrium, and vice versa, *Advanced Quantum Technologies* **2**, 1800043 (2019).
- [32] I. Kovacic, R. Rand, and S. Mohamed Sah, Mathieu's Equation and Its Generalizations: Overview of Stability Charts and Their Features, *Appl. Mech. Rev.* **70**, 020802 (2018).
- [33] R. Mattes, I. Lesanovsky, and F. Carollo, Entangled time-crystal phase in an open quantum light-matter system, arXiv:2303.07725 (2023), 2303.07725.
- [34] J. H. Taylor and K. S. Narendra, Stability regions for the damped mathieu equation, *SIAM Journal on Applied Mathematics* **17**, 343 (1969).
- [35] P. Domokos, P. Horak, and H. Ritsch, Semiclassical theory of cavity-assisted atom cooling, *J. Phys. B* **34**, 187 (2001).